

Influence of the rate of directional crystallization and silicon content on the structure and strength of the Al–Si–Cu alloy

© S.P. Nikanorov, V.N. Osipov, R.B. Timashov, A.V. Chikiryaka

Ioffe Institute, St. Petersburg, Russia
E-mail: osvn@mail.ioffe.ru

Received August 12, 2022

Revised December 19, 2022

Accepted December 28, 2022

The structure and strength of $Al_xSi-2wt.\%Cu$ ($x = 15, 17$ and $20 wt.\%$) alloys obtained by directional solidification at a rate of 0.1 and $0.8 mm/s$ are investigated. It is shown that the tensile strength increases with an increase in the rate of solidification due to a decrease in the size of eutectic silicon and the transformation of its crystal flake into a fine-fiber one. In addition, there was an increase in tensile strength due to an increase of the share of the intermetallic phase, exceeding the reduced tensile strength due to an increase in the amount of the $\alpha-Al$ phase. An increase in the silicon content in the samples during solidification at a rate of $0.1 mm/s$ does not lead to a change in structure and strength. At a higher rate of solidification, there is a reduction of the share of eutectic and a decrease in strength.

Keywords: aluminum alloys, eutectic, structure, tensile strength.

DOI: 10.21883/TP.2023.04.55944.202-22

Introduction

Silumins are aluminum alloys with silicon as the main second component. Cast alloys have a number of advantages: high strength at low specific gravity, high fluidity, high corrosion and wear resistance, relatively low cost. Of particular interest are hypereutectic silumins, in which the silicon content is from 14 to $25 wt.\%$ [1]. Such alloys have increased heat resistance and wear resistance. However, an increase in the silicon content in the Al–Si alloy above the eutectic one ($12.5 wt.\%$) causes a drop in the ultimate strength due to an increase in local stresses on the primary silicon crystals. Therefore, extensive research is currently underway to change the shape and reduce the size of primary bulk and eutectic acicular silicon crystals. These studies are also aimed at finding the possibility of further reducing the coefficient of thermal expansion (the lowest of all silumins), which is necessary when using hypereutectic alloys in internal combustion engines [2,3].

The structure can be modified in various ways [4]. A common variant is to introduce additional chemical elements, mainly phosphorus and strontium [5–10]. Thermal deformation modification is widely used [11]. The possibility of using physical methods for modifying melts is investigated [12]. But it seems to us that it can be economical to modify the structure by changing the rate of solidification. It is known that with an increase in the rate of solidification, the grain size decreases and the shape changes, leading to an increase in the strength of the Al–Si alloy. However, this also increases the porosity of the alloy, especially at rates above $10^4 \mu m/s$ [13]. This is probably why the modification of the structure by changing the solidification rate is rarely used, except for alloy quenching.

It is known that with an increase in the rate of solidification of the Al–Si-alloy, the eutectic point on the state diagram of Al–Si shifts towards a higher silicon content [14]. It has been shown in [15,16] that for an alloy with a composition equal to the composition at the displaced eutectic point at a high crystallization rate, there is a maximum ultimate tensile strength (UTS) and a sharp increase in elongation at fracture. The value of this maximum is greater than the maximum at low rate under quasi-equilibrium conditions. The alloy obtained at the displaced eutectic point has a eutectic microstructure without $\alpha-Al$ dendrites and without primary silicon crystals and, therefore, it becomes possible to obtain hypereutectic alloys with a eutectic microstructure, with increased strength and ductility. In Ref. [15], two-component Al– $15 wt.\% Si$ -alloys with fine-fiber, supermodified structure, with increased strength and high ductility were obtained using the method of directional crystallization at a solidification rate of $1 mm/s$.

Three-component Al–Si–Cu alloys with additional alloying are widely used in industry. Therefore, it is of interest to study the possibility of obtaining a three-component silumin of a hypereutectic composition with increased strength and ductility near the eutectic point, shifted due to an increase in the cooling rate, by analogy with a two-component alloy.

The effect of copper addition to the Al– $12 wt.\% Si$ binary alloy was studied in [17]. The Al– $12 wt.\% Si-4.5 wt.\% Cu$ alloy had a UTS higher than that of the binary base by 37.3% . Ref. [18] investigates the effect of thermal treatment of Al–Si–Cu–Mg alloys on the structure and mechanical properties. The structure of the dendrites of the $\alpha-Al$ phase is characterized by the generally accepted quantity, the secondary dendrite arm spacing (SDAS) (Fig. 1).

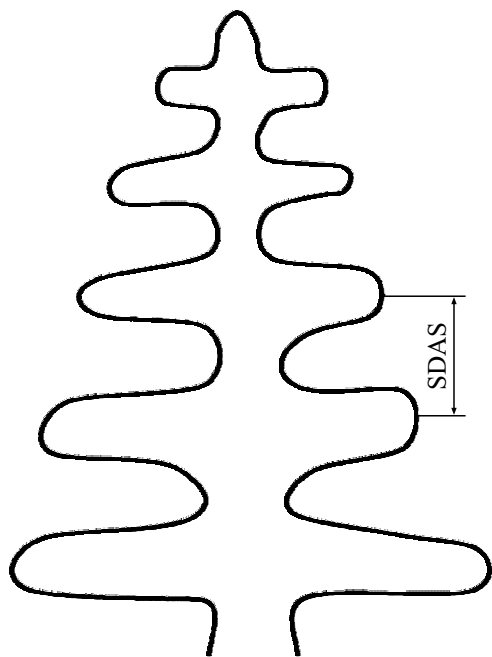


Figure 1. Secondary dendrite arm spacing (SDAS) definition.

It is noted that the SDAS value can be used as a characteristic indicator of the structure and properties of alloys. Increasing SDAS reduces strength and reduces tensile elongation. However, the properties of industrial alloys with SDAS up to $30\mu\text{m}$ can be improved by heat treatment of the melt.

The structure and properties of Al–Si–Cu alloy were studied earlier in Ref. [19]. Samples of Al–9.60 wt.% Si–2.86 wt.% Cu–0.61 wt.% Fe–0.19 wt.% Mn composition were obtained by directional solidification of the melt in a cylindrical crucible with water cooling. Four phases were observed: α , consisting of Al, Si, Cu, Fe, Mg, and β , including Si, Al, Fe, Cu, as well as the eutectic (Al, Si) and Al–Cu. With an increase in the cooling rate, SDAS decreased from 27 to $9\mu\text{m}$, the acicular structure of the eutectic silicon turned into a fibrous one, and the ultimate tensile strength, UTS, increased from 225 to 272 MPa.

Effect of solidification rate and other factors on the microstructure and mechanical properties of Al–10.6 wt.% Si–2.5 wt.% Cu–0.3 wt.% Mg alloy upon crystallization has been studied [20]. Various methods were used: 1) traditional gravity casting, 2) injection molding, 3) double roll continuous casting with cooling, 4) continuous horizontal casting with water drop cooling. A high cooling rate V was used in the case of the last two methods, 255 and 327 K/s respectively. It was estimated based on measuring the SDAS of samples according to the relation $V = 2 \cdot 10^4 (\text{SDAS})^{-2.67}$. The value of UTS and the yield strength σ_{02} increased in the above sequence of methods as $\sigma_{02} = 6.09/(\text{SDAS})^{0.5} + 48.5$. The main reasons for the growth are a decrease in the grain size of α -Al, the transformation of the flake (acicular) structure

Table 1. Composition of studied alloys (wt.%)

Mg	Al	Si	Ti	Mn	Fe	Ni	Cu	Zn
0.80	74.6	14.6	0.3	0.5	1.2	1.1	2.5	0.6
0.9	74.5	17.4	0.1	0.4	0.7	1.08	2.3	0.4
0.5	71.8	20.1	0.2	0.5	1.3	0.8	1.9	0.3

of eutectic silicon into a fibrous one, and a decrease in fiber size. Uniform crystal orientation throughout the ingot, high strength and tensile elongation of an alloy of the same composition as in [20] were observed at high cooling rates (201 K/s) in [21]. Optimal heat treatment regimes were found to further increase the strength and ductility of the alloy.

Studies of Al–Si–Cu-alloys were carried out with rare exceptions on hypoeutectic silumins. The aim of this work was to study the influence of the directional solidification rate and the composition of a hypereutectic three-component alloy on its structure and strength properties.

1. Materials and research methods

From industrial Al–Si–Cu-alloy in a chamotte-graphite crucible at a temperature of about 700°C , initial ingots were grown in the form of ribbons of rectangular cross section by the method of directional crystallization (the Stepanov method) [16]. The melt was preliminarily homogenized at 800°C for about 3 h with periodic stirring. Ribbons with a length of 0.5 m and a cross section of $15 \times 3\text{ mm}$ were drawn from the melt through a shaper with a rectangular hole under air jet cooling. Two draw speeds were used: 0.1 and 0.8 mm/s. Alloy samples were grown both with the original initial content and with the addition of silicon to the melt. Samples 60 mm long with a test part 20 mm long and $3 \times 3\text{ mm}$ in cross section were cut out of the ribbons for structure studies and tensile tests.

The material composition of the grown ribbons was determined by the method of energy diffraction spectroscopy (EDS) with repeated measurements on different parts of the surfaces along the direction of drawing. The silicon content was additionally checked by optical emission spectroscopy both on the longitudinal and cross sections of the ribbons. The mean error in determining the silicon content in the samples, obtained by different measurement methods and in different parts of the samples, did not exceed 3%. Table 1 shows the data obtained by the EDS method. Microstructural analysis of the studied samples was carried out using a Phenom Pro X scanning electron microscope with energy diffraction spectrometer.

The relative area fractions occupied by the individual phases of the alloys under study in the microstructure photographs were determined by the number of image pixels occupied by each phase and having a certain contrast. Tensile tests were carried out on an Instron 1342 universal

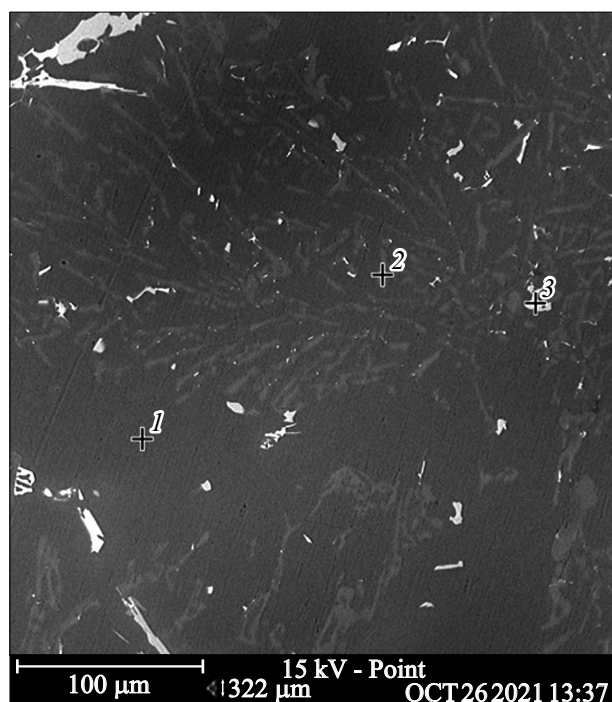


Figure 2. Electron microscopic image of the Al–15 wt.% Si–2 wt.% Cu alloy obtained by directional crystallization by the Stepanov method at a solidification rate of 0.1 mm/s (1 — α -Al solid solution; 2 — eutectic; 3 — intermetallic compounds).

testing machine at a clamping speed of $6 \mu\text{m} \cdot \text{s}^{-1}$. This corresponds to a relative strain rate of $3 \cdot 10^{-4} \text{s}^{-1}$.

2. Results

2.1. Microstructure

An electron microscopic image of the microstructure of the Al–15 wt.% Si–2 wt.% Cu alloy sample obtained at a solidification rate of 0.1 mm/s is shown in Fig. 2. Three structural phases can be distinguished: α -Al solid solution (marked with point 1), eutectic (point 2), and intermetallic compounds formed by aluminum and silicon with transition metals (point 3). The elemental composition at the marked points, determined by the EDS method, is given in Table 2.

An electron microscopic image of the microstructure of the Al–15 wt.% Si–2 wt.% Cu alloy sample obtained at a solidification rate of 0.8 mm/s is shown in Fig. 3. One can distinguish α -Al solid solution (dark gray), light gray eutectic consisting of eutectic silicon and α -Al, and white intermetallics (point 5) containing Al, Si, alloying metals (Cu, Ni, Fe, Mn), and alkaline earth metal (Mg) according to the results of EDS-analysis (Table 3).

The effect of solidification rate and silicon content on the structure of the alloy was also studied using optical microscopy. Figure 4 shows the microstructure of an alloy with 15 wt.% of silicon obtained at a solidification rate of

Table 2. The content of elements (wt.%) at the points of the phases microstructure of the Al–15 wt.% Si–2 wt.% Cu alloy obtained at a rate of 0.1 mm/s

Nº of point (Fig. 1)	Al	Si	Cu	Ni	Fe	Mn
1	94.62	5.38	–	–	–	–
2	47.21	52.79	–	–	–	–
3	68.83	13.64	1.84	1.60	8.36	5.73

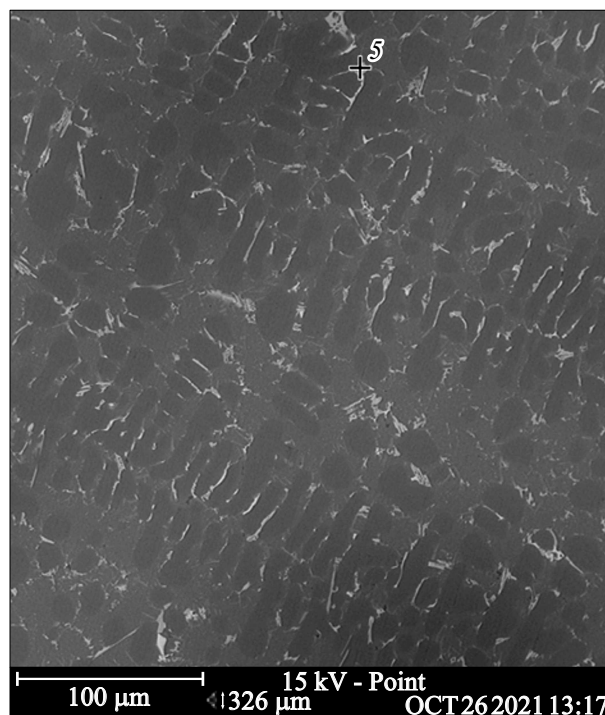


Figure 3. An electron microscopic image of the structure of the Al–15 wt.% Si–2 wt.% Cu alloy obtained at a solidification rate of 0.8 mm/s (point 5 — intermetallics).

Table 3. Content of elements (wt.%) at the point of the phase microstructure of the Al–15 wt.% Si–2 wt.% Cu alloy obtained at a rate of 0.8 mm/s

Nº of point (Fig. 2)	Al	Si	Cu	Ni	Fe	Mn	Mg
5	75.5	7.63	5.90	6.20	2.1	1.33	1.25

0.1 and 0.8 mm/s at two magnification scales (Fig. 4, *a, c* and Fig. 4, *b, d* respectively). In both cases, three structural phases are observed: α -Al dendrites (white color), eutectic (a mixture of black-colored eutectic silicon and α -Al), and intermetallic compounds (clearly observed in Fig. 4, *c*, light grey). It is seen that with an increase in the solidification rate, the dendrites become thinner. The eutectic with silicon in the form of bundles of needles (traces of the intersection of flake plates by the cut plane) up to $100 \mu\text{m}$ in length

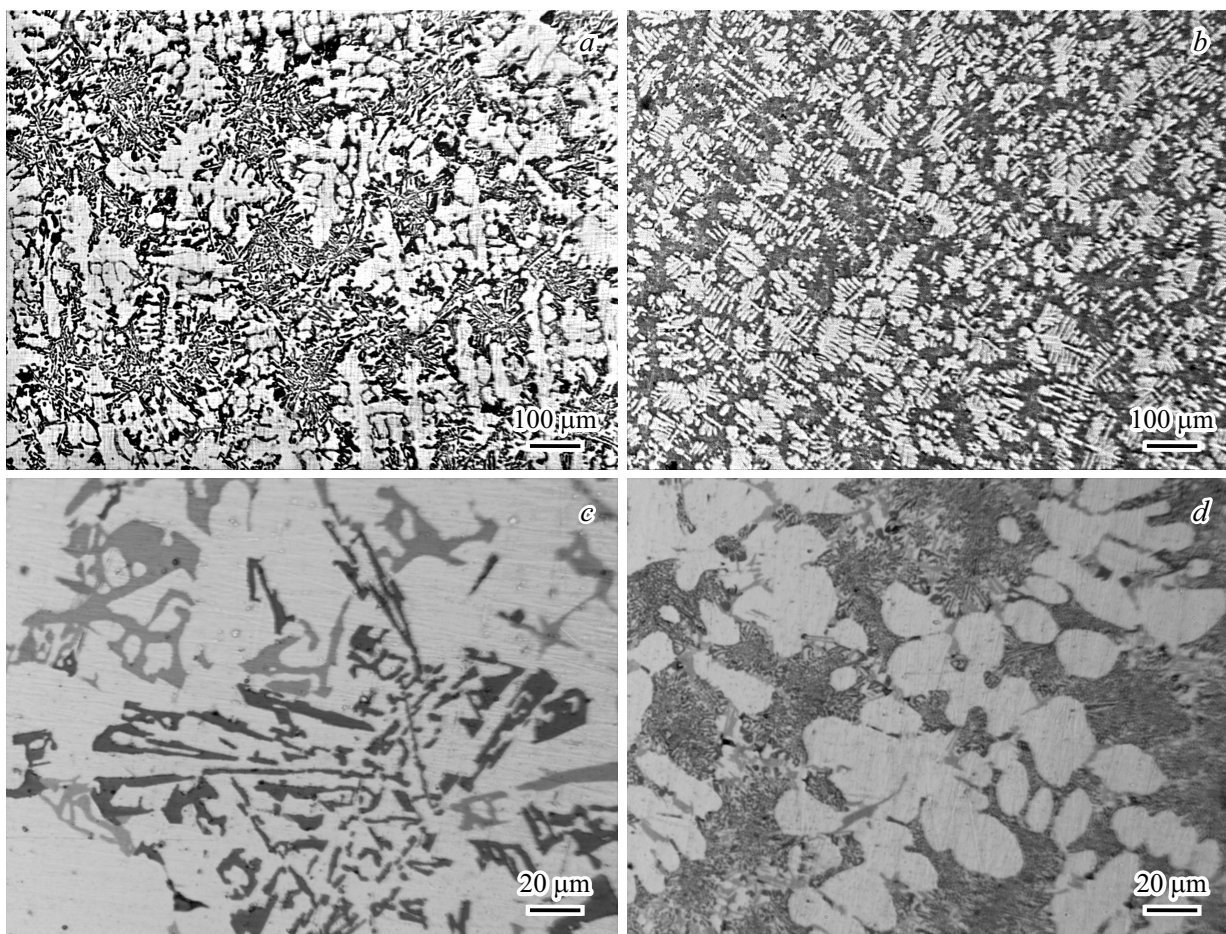


Figure 4. Effect of pulling rate on the structure of Al–15 wt.% Si–2 wt.% Cu at two image magnifications. The rate of solidification: *a, c* — 0.1; *b, d* — 0.8 mm/s.

Table 4. Structural parameters of an alloy with 15 wt.% of silicon at different solidification rates

Alloy	Solidification rate, mm/s	SDAS, μm	Phase area in sample section, %		
			α -Al	Intermetallics	Eutectics
Al–15 wt.%	0.1	57	37.7	3.5	58.8
Si–2 wt.% Cu	0.8	18	49.24	5.4	45.4

at a solidification rate of 0.1 mm/s becomes fine-fibered, optically unresolvable at a rate of 0.8 mm/s. Such a character of the transformation of the flake form of eutectic silicon into fine-fibered one, both in double and triple silumins with an increase in the cooling rate was observed in a number of papers [15,20–23]. It should be noted that at a lower rate, eutectic silicon needles form a star-shaped multiray structure (Fig. 4, *c*). The authors of Ref. [24] believe that such formations are primary silicon.

The relative proportions of areas occupied by each of the phases at different solidification rates are given in Table 4. An increase in the proportion of α -Al and intermetallics with an increase in the rate of solidification can be noted. The table also reflects the decrease in the SDAS

value with an increase in the solidification rate from 0.1 to 0.8 mm/s by 70%.

The effect of silicon content on the structure of the alloy under study is shown in Fig. 5. It can be seen that at a solidification rate of 0.1 mm/s, the structure of the Al–15 wt.% Si–2 wt.% Cu and Al–20 wt.% Si–2 wt.% Cu alloy phases is the same (Fig. 5, *a, c*). In the case of a velocity of 0.8 mm/s, a change in the eutectic microstructure is noticeable. In the eutectic of the Al–20 wt.% Si–2 wt.% Cu alloy, a large number of α -Al grains are seen in the form of small inclusions of various shapes (Fig. 5, *b, d*).

Table 5 shows the area fractions and SDAS phases of an alloy with different silicon contents obtained at the same solidification rate. One can see an increase in the proportion

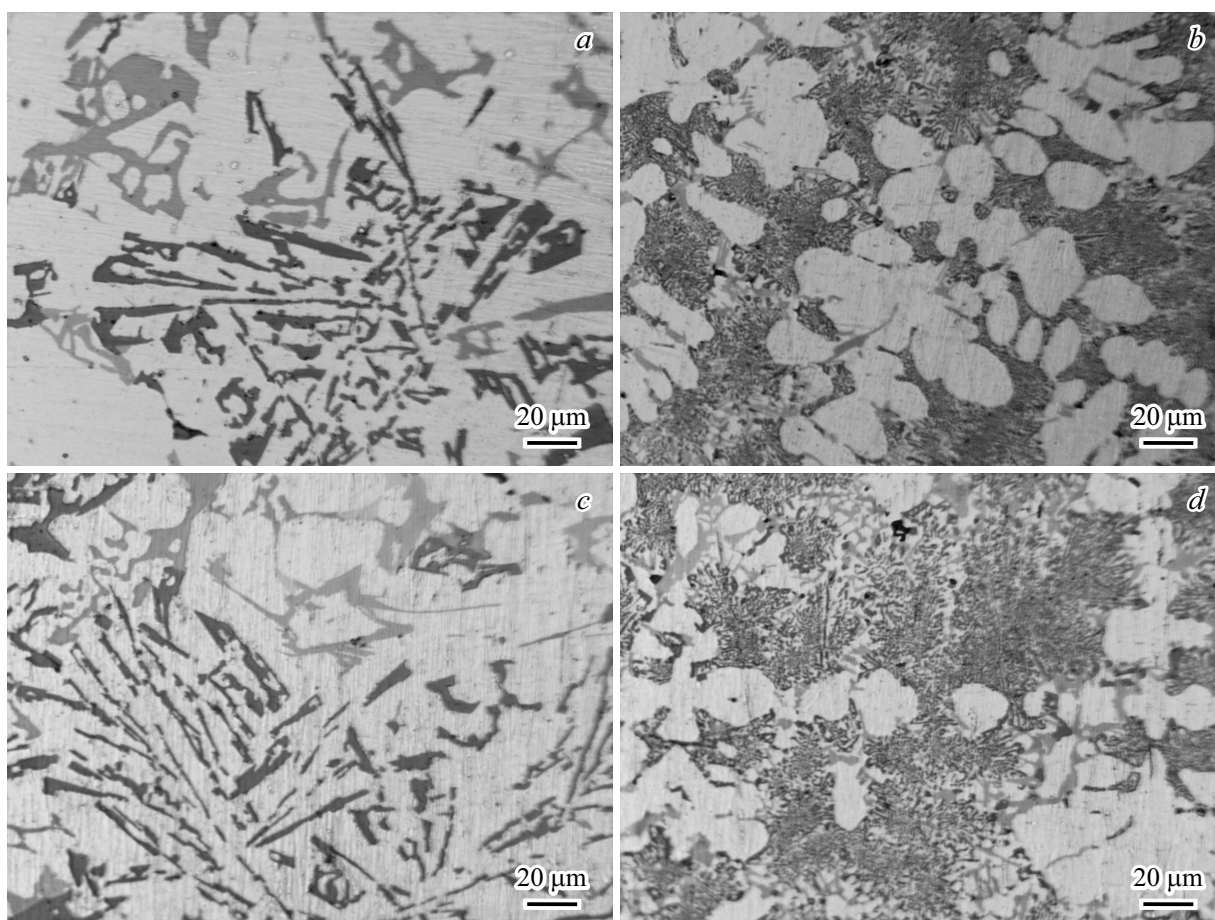


Figure 5. Influence of Si content in Al- x Si-2.0 wt.% Cu alloy on the structure: a, b — $x = 15$ wt.% Si; c, d — $x = 20$ wt.% Si at solidification rate: a, c — 0.1; b, d — 0.8 mm/s.

Table 5. Alloy structure parameters at different silicon content

Alloy	Solidification rate, mm/s	SDAS, μm	Phase area in sample section, %		
			α -Al	Intermetallics	Eutectics
Al-15 wt.% Si-2 wt.% Cu	0.8	18	49.24	5.4	45.4
Al-20 wt.% Si-2 wt.% Cu	0.8	18	55.6	6.6	37.8

of the α -Al phase and intermetallics at an appropriate decrease in the proportion of eutectics in the microstructure. The SDAS value does not change within the measurement error (10%).

2.2. Strength

Fig. 6 shows a diagram of ultimate tensile strength (UTS) of samples with different silicon content obtained at two solidification rates. The average values of measurements for three samples for each composition are given, except for the alloy with 20 wt.% Si. Brittle fracture was observed in samples of this composition. It follows from the diagrams in Fig. 6 that an increase in the solidification rate from 0.1

to 0.8 mm/s leads to a significant increase in UTS for samples of the same composition. At the same time, an increase in the silicon content from 15 to 20 wt.% causes a noticeable decrease in the ultimate strength at a solidification rate of 0.8 mm/s, and at a rate of 0.1 mm/s, these changes are insignificant.

The relative sample elongation upon fracture was 4%.

3. Results and discussion

In contrast to Al-Si hypereutectic binary alloys, primary silicon crystals are not observed in Al-Si-Cu hypereutectic ternary alloys studied here. Only upon solidification at a slower rate, 0.1 mm/s, star-shaped structures are formed,

Table 6. Comparison of UTS of alloys obtained by different methods

Alloy	UTS, MPa		
	Non-modified	+0.04 wt.% Sr	+1.0 wt.% Ce
LM30, casting [10]*	155 ± 5	160 ± 5	190 ± 10
LM30, heat treatment [10]	245 ± 5	250 ± 10	285 ± 5
Al–15 wt.% Si–2 wt.% Cu, directional crystallization	279	–	–

Note. * — composition LM30: Al–16 wt.% Si–3.5 wt.% Cu.

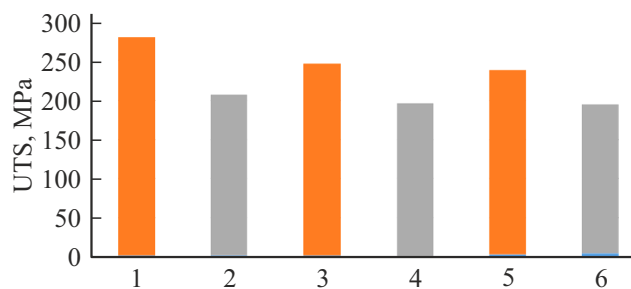


Figure 6. Ultimate Tensile Strength (UTS) as a function of solidification rate and silicon content (solidification rate: column 1, 3, 5 — 0.8; 2, 4, 6 — 0.1 mm/s; Si content: column 1, 2 — 15; 3, 4 — 17; 5, 6 — 20 wt.%).

which in Ref. [24] are presumably referred to primary silicon crystals. The studied material contains a number of impurities, which can be the centers of nucleation of primary α -Al dendritic crystals. The growth of α -Al both in the presence and in the absence of primary silicon in hypereutectic silumins was observed in a number of papers. The formation of α -Al dendritic crystals together with eutectic and primary silicon in a hypereutectic Al–20 wt.% Si alloy with the addition of copper at a cooling rate of 16.2 K/s was observed in Ref. [17]. In Ref. [25], aluminum alloys with silicon content from 13 to 18 wt.% and Cu content 1.0 wt.% obtained at cooling rate 1.0 K/s, had a structure, consisting of α -Al and eutectics.

In the entire range of silicon content studied in this work, the samples consisted of α -Al dendrites, eutectics, and intermetallic compounds. The solidification of these melts occurs with significant supercooling, since they contain Mn, Fe, Cu, Zn, Mg, which have a strong effect on the nature of solidification [26]. Indeed, the estimate of the average eutectic solidification temperature for 15, 17 and 20 wt.% Si alloys at the above copper and impurity content according to the equation proposed by Gruzleski [26] yielded a value of 564°C. The eutectic temperature of the two-component Al–12.5 wt.% Si alloy is 577°C. In addition, the formation of one eutectic without primary crystals in the Al–15 wt.% Si alloy occurs at a rate of 1 mm/s [16], which corresponds to supercooling of the melt about 12°C [27]. Strong supercooling due to the modifying effect of an additional element, copper and impurities, as well as a

high solidification rate, can cause a shift in the eutectic point towards higher silicon content. The value of ultimate strength with increasing silicon content in binary silumins increases to a eutectic composition. A decrease in the ultimate strength with an increase in the silicon content in binary silumins occurs only above the eutectic point. From the data of the present study on the strength of the alloy, it can be assumed that the maximum amount of silicon in the eutectic of the ternary alloy under study is achieved at a silicon content below or equal to 15 wt.% Si. Such a silicon content in the Al–15 wt.% Si binary alloy is observed at a displaced eutectic point at a solidification rate of 1 mm/s [28].

The increase in UTS at a higher solidification rate of the alloy with 15 wt.% Si occurs due to an increase in the strength of the eutectic as a result of the transformation of a coarse, acicular (in the bulk flake) structure into a denser, fine-fibered, optically difficult to resolve structure and additionally due to increasing the amount of the intermetallic phase (Fig. 4, *a, b* or 4, *c, d*). The contribution to the increase in the strength of the alloy due to the refinement of the eutectic and the increase in the volume of the intermetallic phase from 3.5 to 5.4% with an increase in the solidification rate from 0.1 to 0.8 mm/s exceeds the contribution to the drop in strength from a decrease in the volume of the eutectic from 58.8 to 45.4% and the corresponding increase in the volume of the α -Al dendritic structure from 37.7 to 49.2% (Table 4). In this case, a decrease in the SDAS value, which is determined by the structure rather than the volume of phases, is observed from 57 to 18 μ m (Fig. 7).

With an increase in the silicon content in the alloy from 15 to 20 wt.% for a solidification rate of 0.1 mm/s (Fig. 5, *a, c*), the structure character does not change and the strength remains practically unchanged, too. At a solidification rate of 0.8 mm/s, an increase in the silicon content does not cause a noticeable change in the overall structure of the alloy. However, an increase in the amount of microscopic precipitates of the α -Al phase outside the dendrites in the eutectic body is observed. This leads to a decrease in the proportion of eutectics and an increase in the amount of the α -Al phase in the microstructure. The SDAS value does not change (18 μ m), since the structure of each phase does not change, only volume fractions change. Ultimate strength

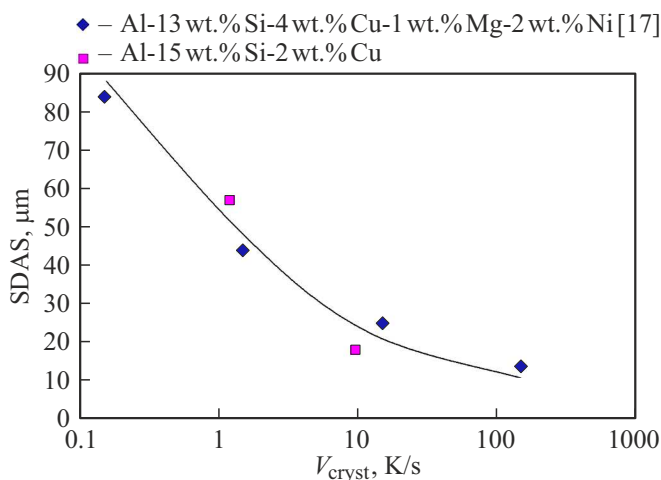


Figure 7. Dependence of SDAS on alloy solidification rate.

increases by 47% due to an increase in the proportion of intermetallics.

The strength of the samples obtained exceeds the strength of samples of alloys similar in composition obtained by traditional casting in a metal crucible without heat treatment [29]. Traditional casting can provide the strength of the Al–Si–Cu alloy reported here only after modifying the alloy with cerium and additional heat treatment (Table 6). It can be expected that additional modification of an alloy produced near the silicon-shifted eutectic point will result in a higher strength compared to an alloy produced by conventional casting.

Conclusion

An increase in the solidification rate of Al– x Si–2 wt.% Cu alloy ($x = 15, 20$ wt.%) from 0.1 to 0.8 mm/s causes the transformation of the rough flake structure of the eutectic into a stronger, fine-fibered, optically unresolvable structure. The increase in the strength of the alloy due to the structural strengthening of the eutectic and the increase in the volume of the intermetallic phase from 3.5 to 5.4% exceeds the contribution to the alloy softening due to a decrease in the volume of the eutectic and an increase in the volume of the α -Al dendritic structure by 43 MPa. In this case, there is a decrease in the SDAS value, which is determined by the structure of the phases rather than by the volume, from 57 to 18 μm .

When increasing the silicon content in the Al–Si–Cu alloy from 15 to 20 wt.% and keeping the solidification rate at 0.1 mm/s, the structure character and strength do not change. At a solidification of the alloy with the rate of 0.8 mm/s, an increase in the silicon content does not cause a noticeable change in the general structure of samples. However, an increase in the proportion of microscopic precipitates of the α -Al phase outside the

dendrites in the eutectic body is observed. An increase in the silicon content in the alloy causes a decrease in the volume fraction occupied by the eutectic over the cross-sectional area by 7.6%, an increase in the area occupied by intermetallic compounds by 22% and α -Al phase — by 13%. The SDAS value remains constant at 18 μm . The value of UTS grows due to an increase in the proportion of intermetallic compounds.

The content of silicon in the eutectic near the shifted eutectic point at a solidification rate of 0.8 mm/s is about 15 wt.%.

The ultimate tensile strength, 275 MPa, obtained by the method of directional crystallization in Al–Si–Cu alloy samples, exceeds the strength of alloys obtained by traditional casting.

Conflict of interest

The authors declare that they have no conflict of interest.

References

- [1] G.B. Stroganov, V.A. Rotenberg, G.B. Gershman. *Splavy alyuminiya s kremniyem* (Metallurgiya, M., 1977) (in Russian)
- [2] M.V. Popova, V.V. Ushakova, Z.A. Luzyanina. *Izv. vuzov. Chernaya metallurgiya*, **8**, 55 (1995). (in Russian).
- [3] M.V. Popova, V.V. Ushakova, Z.A. Luzyanina. *Izv. vuzov. Chernaya metallurgiya*, **6**, 81 (1994) (in Russian).
- [4] V. Vijeesh, K. Narayan Prabhu. *Trans. Indian Inst. Met.*, **67** (1), 1 (2014). DOI: 10.1007/s12666-013-0327-x
- [5] V.N. Osipov. *ZhTF*, **92** (9), 1365 (2022) (in Russian). DOI: 10.21883/JTF.2022.09.52928.42-22
- [6] Yu.Ya. Zilberg, N.M. Khrushcheva, G.B. Gershman. *Alyuminiyevyye splavy v traktorostroyenii* (Mashinostroyeniye, M., 1971) (In Russian)
- [7] T.N. Smirnova. *Modifitsirovaniye zaevtekticheskikh siluminov. V sb.: Modifitsirovaniye siluminov*. Pod red G.V. Samsonova. Nauk. dumka, Kiev (1970), p. 25. (in Russian).
- [8] A.P. Gudchenko, I.M. Zalivanova. *Liteynoye proizvodstvo*, **12**, 30 (1972) (in Russian).
- [9] L.P. Seleznev, T.P. Borovitskaya, E.V. Kuznetsova. *Nauchnyye trudy Instituta Giprotsvetmetobrabotka*, **58**, 63 (1978) (in Russian).
- [10] Y.C. Lin, Shun-Cun Luo, Jian Huang, Liang-Xing Yin, Xing-You Jiang. *Mat. Sci. Eng. A* **725**, 530 (2018). DOI: 10.1016/j.msea.2018.04.049
- [11] S. Hegde, K.N. Prabhu. *J. Mater.Sci.*, **43** (9), 3009 (2008). DOI: 10.1007/s10853-008-2505-5
- [12] K.V. Nikitin. *Modifitsirovaniye i kompleksnaya obrabotka siluminov* (Samarskiy gosudarstvennyy tekhnicheskii universitet, Samara, 2016) (in Russian)
- [13] G.K. Sigworth. *Int. J. Metalcast.*, **2** (2), 19 (2008). DOI: 10.1007/BF03355425
- [14] L.F. Mondolfo. *Aluminum Alloys: Structure and Properties* (London, Butterworth Ltd., 1976)
- [15] A.I. Averkin, B.N. Korchunov, S.P. Nikanorov, V.N. Osipov. *Tech. Phys. Lett.*, **42** (2), 201 (2016). DOI: 10.1134/S106378501602019X

- [16] S.P. Nikanorov, L.I. Derkachenko, B.K. Kardashev, B.N. Korchunov, V.N. Osipov, V.V. Shpeizman. Phys. Solid State, **55** (6), 1207 (2013). DOI: 10.1134/S1063783413060255
- [17] C.G. Shivarprasad, S. Narendranath, Vijay Desai, Sujeeth Swami, M.S. Ganesha Prasad. Proc. Mat. Sci., **5**, 1368 (2014). DOI: 10.1016/j.mspro.2014.07.454
- [18] L. Aguilera Luna, H. Mancha Molinar, M.J. Castro Roman, J.C. Escobedo Bocardo, M. Herrera Trejo. Mater. Sci. Eng. A, **561**, 1 (2013). DOI: 10.1016/j.msea.2012.10.064
- [19] H. Borkar, S. Seifeddine, A.E.W. Jarfors. Sol. St. Fen., **287**, 18 (2019). DOI: 10.4028/www.scientific.net/SSP.287
- [20] M. Okayasu, Y. Ohkura, S. Takeuchi, H. Ohfuji, T. Shiraishi. Mat. Sci. Eng. A, **543**, 185 (2012). DOI: 10.1016/j.msea.2012.02.073
- [21] M. Okayasu, S. Takeuchi, T. Ochi. Int. J. Cast Metal. Res., **30** (4), 217 (2017). DOI: 10.1080/13640461.2017.1286556
- [22] T. Hosch, L.G. England, R.E. Napolitano. J. Mater. Sci., **44** (18), 4892 (2009). DOI: 10.1007/s10853-009-3747-6
- [23] L. Tian, Y. Guo, J. Li, F. Xia, M. Liang, Y. Bai. Materials, **11** (7), 1230 (2018). DOI: 10.3390/ma11071230
- [24] O.A. Atasoy, F. Yilmaz, R. Elliott. J. Cryst. Growth, **66** (1), 137 (1984). DOI: 10.1016/0022-0248(84)90084-8
- [25] R. Wang, W. Lu. Int. J. Mater. Sci. Appl., **5** (6), 277 (2016). DOI: 10.11648/j.ijmsa.20160506.17
- [26] M.B. Djurdjevic. Vojnotehnički Glasnik/Military Technical Courier, **60** (1), 152 (2012). DOI: 10.5937/VojnotehnickiGlasnik
- [27] D.C. Jenkinson, L.M. Hogan. J. Cryst. Growth, **28** (2), 171 (1975). DOI: 10.1016/0022-0248(75)90233-X
- [28] S.P. Nikanorov, V.N. Osipov, L.I. Regel. J. Mater. Eng. Perform., **28**, 7302 (2019). DOI: 10.1007/s11665-019-04414-3
- [29] V. Vijeesh, M. Ravi, K. Narayan Prabhu. Mater. Perform. Character., **2** (1), 296 (2013). DOI: 10.1520/MPC20120007

Translated by Ego Translating